Published in final edited form as:
Biomaterials. 2012 June ; 33(18): 4773–4782. doi:10.1016/j.biomaterials.2012.03.032.

Surface conjugation of triphenylphosphonium to target poly(amidoamine) dendrimers to mitochondria

Swati Biswas, **Namita S. Dodwadkar**, **Aleksandr Piroyan**, and **Vladimir P. Torchilin***
Center for Pharmaceutical Biotechnology and Nanomedicine, Northeastern University, 312 Mugar Hall, 360 Huntington Ave. Boston, MA 02115, USA

Abstract

Dendrimers have emerged as promising carriers for the delivery of a wide variety of pay-loads including therapeutic drugs, imaging agents and nucleic acid materials into biological systems. The current work aimed to develop a novel mitochondria-targeted generation 5 poly(amidoamine) (PAMAM) dendrimer (G(5)-D). To achieve this goal, a known mitochondriotropic ligand triphenylphosphonium (TPP) was conjugated on the surface of the dendrimer. A fraction of the cationic surface charge of G(5)-D was neutralized by partial acetylation of the primary amine groups. Next, the mitochondria-targeted dendrimer was synthesized via the acid-amine-coupling conjugation reaction between the acid group of (3-carboxypropyl)triphenyl-phosphonium bromide and the primary amines of the acetylated dendrimer (G(5)-D-Ac). These dendrimers were fluorescently labeled with fluorescein isothiocyanate (FITC) to quantify cell association by flow cytometry and for visualization under confocal laser scanning microscopy to assess the mitochondrial targeting *in vitro*. The newly developed TPP-anchored dendrimer (G(5)-D-Ac-TPP) was efficiently taken up by the cells and demonstrated good mitochondrial targeting. *In vitro* cytotoxicity experiments carried out on normal mouse fibroblast cells (NIH-3T3) had greater cell viability in the presence of the G(5)-D-Ac-TPP compared to the parent unmodified G(5)-D. This mitochondriatargeted dendrimer-based nanocarrier could be useful for imaging as well as for selective delivery of bio-actives to the mitochondria for the treatment of diseases associated with mitochondrial dysfunction.

Keywords

Dendrimer; TPP; Conjugation; Mitochondrial targeting; Cytotoxicity

1. Introduction

Dendrimers are hyperbranched, monodisperse, tree-like synthetic macromolecules with three distinct components that include a central core, repeated branches and a large number of functional groups on the surface [1–3]. Since their discovery, dendrimers have been studied extensively and hold promise as a nanocarrier for site-specific delivery of therapeutic and imaging agents due to their unique properties including multiple surface attachment sites, good biocompatibility, tunable size, spherical shape and monodispersity [4–8]. The ability to functionalize the surface groups with various moieties makes dendrimer a versatile pharmaceutical nanocarrier. PAMAM dendrimers have wide application as non-viral gene delivery vectors [9–13]. PAMAM with a high generation number (G > 5) have

*Corresponding author. Tel.: +1 617 373 3206; fax: +1 617 373 7509. v.torchilin@neu.edu (V.P. Torchilin).

Appendix A. Supplementary material
Supplementary material associated with this article can be found, in the online version, at doi:10.1016/j.biomaterials.2012.03.032.

high cationic surface charge, which can spontaneously bind nucleic acids by electrostatic interaction [1,14–17] . The PAMAM-nucleic acid complexes with a net positive charge promote endosomal escape and allow efficient transfection [8,17].

Dendrimers have many applications in drug delivery to improve solubility, biocompatibility and pharmacokinetic properties of drugs [1]. They are advantageous due to their ability to encapsulate drugs in the core as well as chemically conjugate many molecules of drugs on the surface. The endless possibilities for chemical modifications also allow the incorporation of many other functionalities such as solubilizing groups including PEG, ligands for target cell recognition and imaging agents. Unlike self-assembled nanocarriers, which are energetically meta-stable depending on concentration, dendrimers maintain their structural integrity in biological systems [9].

Targeting therapeutics to intracellular organelles of interest could be very effective in maximizing the drug effect and minimizing side effects [18]. However, intracellular delivery and subsequent targeting to specific cellular compartments is challenging, especially for macromolecular drug delivery systems, due to a cell membrane that prevents their spontaneous entrance and that nanoparticles are taken up primarily by energy-dependent endocytosis [18]. The cell association of nanoparticles can be enhanced with cationic lipids or surface conjugation with short cell-penetrating cationic lysine (Lys)- or arginine (Arg)-rich peptides such as TATp and Antp [18]. Endosome disruption allows delivery of nanoparticles or their cargo into the cytoplasm. The free tertiary amine groups in the PAMAM dendrimer promote an efficient endosomal escape as well [19]. In general, there is a definite possibility to satisfy the need for drug carriers targeted to specific intracellular compartments and organelles, rather than achieving just a cell-surface association or intracellular localization.

The possibility of targeting drugs/nanocarriers to the mitochondria to facilitate drug action has gained much attention recently. There has been increasing evidence that mitochondrial dysfunction contributes to a variety of human disorders including neurodegenerative and neuromuscular diseases, diabetes, obesity and cancer [20–23]. Mitochondria play a pivotal role in the initiation of apoptosis [24,25]. Mutation in mitochondrial DNA (mtDNA) appear to be responsible for the onset of many diseases [22,26]. Therefore, attempts to correct defects in mitochondrial signal transduction pathways and/or mtDNA itself make mitochondria-targeted drug and gene therapy highly desirable.

Numerous investigators have attempted to deliver a therapeutic cargo to the mitochondria. Mitochondria have been targeted for the delivery of small molecules including antioxidants to decrease cardiac ischemia-reperfusion injury and Friedreich’s ataxia [27–30]. Mitochondria-targeted liposomes delivered potent anticancer drugs to the mitochondria resulting in an enhanced therapeutic effect [20,31–34]. Targeted delivery of DNA to the mitochondrial compartment has been achieved by mitochondriotropic cationic vesicles and by conjugating a mitochondrial targeting signal peptide to DNA [35,36].

Various strategies have been designed to impart a mitochondria-targeting ability. Triphenylphosphonium (TPP), a cation with sufficient lipophilicity and delocalized positive charge, promoted efficient in accumulation in the mitochondria by reducing the free energy change on movement from an aqueous to a hydrophobic environment in response to the mitochondrial membrane potential [32]. Conjugating a TPP group to various small molecules or even to a drug delivery system can facilitate their mitochondrial targeting [27,28,31,34,37–39]. A mitochondria-targeted G(4)-PAMAM dendrimer-based imaging agent was synthesized by conjugation of a small molecule ligand for translocator protein, which spans the mitochondrial membrane [40].

The present study describes the design, synthesis, cell uptake, mitochondrial targeting and cytotoxicity of a TPP-conjugated, acetylated, fluorescently-labeled G(5)-PAMAM dendrimer. G(5)-D was acetylated to reduce the non-specific cellular interactions, which could lead to cytotoxicity. Fluorescein isothiocyanate (FITC) conjugation allowed visualization with fluorescence microscopy to assess its trafficking towards mitochondria.

2. Materials and methods

2.1. Materials

A PAMAM dendrimer, 5 wt % solution in methyl alcohol, acetic anhydride, *N,N'*-Disuccinimidyl carbonate (DSC), (3-Carboxypropyl)triphenyl-phosponium bromide (CTPB), *N*-(3-Dimethylaminopropyl)-N'-ethylcarbodiimide hydrochloride (EDCI), N-hydroxysuccinimide (NHS), *trans* indole acrylic acid and triethylamine (TEA) were purchased from Sigma–Aldrich (St Louis, MO). NHS-Fluorescein was obtained from Pierce (Rockford, IL). Cellulose ester (CE) dialysis membrane tubing 10 kDa MWCO was purchased from Fisher Scientific (Fair Lawn, NJ).

The methanolic solution of G(5)-PAMAM dendrimer was aliquoted in pre-weighed vials, solvent evaporated and the thick viscous liquid was freezedried. The weight of the dendrimers was obtained from the weighed vials. Solid dendrimers were dissolved in a solvent appropriate for the reaction conditions. For cell studies, all dendrimers were dissolved in water at a concentration of 1 mM.

2.2. Cell culture

Human cervical carcinoma (HeLa), MCF-7 human breast cancer cells, 4T1 murine mammary carcinoma and mouse normal fibroblast cells (NIH-3T3) were purchased from the ATCC (Manassas, VA). HeLa cells were chosen for cellassociation and intracellular trafficking experiments (since cancer cells are expected to be the therapeutic target), while fibroblast and other cancer cells were used to determine the cytotoxicity. Dulbecco's modified Eagle's media (DMEM), fetal bovine serum (FBS), and penicillin-streptomycin solution were obtained from CellGro (Kansas City, MO). Mitotracker deep red FM and Hoechst 33342 were purchased from Molecular Probes, Inc. (Eugene, OR). *Para* formaldehyde was from Electron Microscopy Sciences (Hatfield, PA). Fluoromount-G was from Southern Biotech (Birmingham, AL). The CellTiter 96® AQueous One Solution Cell Proliferation Assay kit was purchased from Promega (Madison, Wl). The trypan blue solution was obtained from Hyclone (Logan, UT).

Both cell lines were grown in DMEM, supplemented with 10% FBS, 100 IU/mL of penicillin, streptomycin and 250 ng/mL amphotericin-B at 37 °C and 5% CO_2.

2.3. Synthesis of FITC-labeled dendrimer FITC-G(5)-D

Into the solution of G(5)-D (200 mg) in phosphate buffered saline (PBS) at pH 8, was added NHS-fluorescein (3.3 mg) dissolved in dimethylformamide. The reaction mixture was stirred at room temperature for 2 h and dialyzed against water using a cellulose ester membrane (MWCO 10 kDa) overnight with two water changes. The dialysate was frozen in a pre-weighed vial, and lyophilized to obtain the solid product.

2.4. Synthesis of FITC-labeled acetylated dendrimer, FITC-G(5)-D-Ac

Into the solution of FITC-G(5)-D (50 mg) in 2 mL of methanol, TEA (20 μL) was added. Acetic anhydride (16.2 μL) dissolved in 50 μL of methanol was added drop-wise into the FITC-G(5)-D/TEA solution. The reaction mixture was stirred for 24 h. Methanol/TEA was evaporated and the crude reaction mixture was dialyzed against water using 10,000 MWCO

cellulose ester membrane. The dialysate was frozen and lyophilized to obtain a solid product and stored as solid until further synthesis.

2.5. Synthesis of FFTC-labeled acetylated TPP-modified dendrimer FITC-G(5)-D-Ac-TPP

For the modification of dendrimers, CTPB was activated using *N,N'*-disuccinimidyl carbonate. Into the solution of CTPB (50 mg, 0.12 mMol) in chloroform, 1.1 mol equivalents of DSC (32.8 mg, 0.13 mMol), dissolved in 500 μL of chloroform was added at 0 °C. The reaction mixture was stirred at room temperature overnight. The chloroform was evaporated, and the system was freeze dried. The reaction mixture was dissolved in DMF at a concentration of 50 mg/mL, stored at −20 °C and used in the next reaction without additional purification. FITC-G(5)-D-Ac (20 mg, 0.65 μMol) was dissolved in PBS, pH 8, and a 5 mol equivalent excess of the NHS-activated CTPB (1.63 mg) solution in DMF was added. The reaction mixture was stirred at room temperature for 4 h and dialyzed against water using cellulose ester membrane (MWCO 10 kDa). The dialysate was frozen, lyophilized to obtain a solid, fluffy powder, which was dissolved in water at a concentration of 1 mM and stored at −80 °C (G)-5-Ac and G(5)-D-Ac-TPP were also synthesized following the above procedure for cytotoxicity studies.

For characterization, ^{1}H nuclear magnetic resonance (NMR) spectroscopy was performed using Varian 400 MHz spectroscope. The dendrimers were dissolved in *d*-DMSO, and a 5–10 mg/mL solution was used. Matrix-assisted laser desorption ionization time of flight (MALDI–TOF) mass spectrometry was performed using a Voyager-DE STR mass spectrometer. *Trans* indole acrylic acid was used as a matrix at 10 mg/mL in DMSO. The plate was spotted with 1 μL of a 10:1 solution of matrix and dendrimers.

2.6. Cell-association of dendrimers estimated by FACS analysis

After the initial passage in tissue culture flasks, approximately 200,000 HeLa cells were seeded in 6-well tissue culture plates. On the next day, the cells were incubated with 2 mL of 0.5 μM solution of F1TC-G(5)-D, FITC-G(5)-D-Ac, FITC-G(5)-D-Ac-TPP in serum-free media for 1 h and 4 h incubation periods. The media was removed, the cells washed several times, gently scraped, suspended in 1 mL PBS and then centrifuged at 1000 RPM for 5 min. The cell pellet was suspended in cold PBS, pH 7.4 before analysis using a BD FACS Caliber flow cytometer. The cells were gated using forward (FSC-H)-versus side-scatter (SSC-H) to exclude debris and dead cells before analysis of 10,000 cell counts. The representative histogram and the statistics to obtain the geometric mean of fluorescence for each cell sample were performed using BD Cell Quest Pro Software.

2.7. Intracellular uptake by confocal laser scanning microscopy

The following method was used for experiments involving the visualization of cells under the confocal microscope. After the initial passage in tissue culture flasks, HeLa cells were grown on cover slips placed in 6-well tissue culture plates in complete media. After the cells reached the 60–70% confluence, the medium was removed. The cells were incubated with FITC-labeled dendrimer solutions (1 μM) for 4 h in serum-free media. After the incubation, the cells were washed with PBS and the cover slips mounted cell-side down on glass slides with fluorescence-free glycerol-based mounting medium (Fluoromount-G) and viewed with a Zeiss Confocal Laser Scanning Microscope (Zeiss LSM 700) equipped with FITC filter for *in vitro* imaging. The FITC-filter (ex. 450–505 nm, em. 515–545 nm) was used for the visualization of dendrimer-dosed cells. z-Stacked images (z 1–15, slice thickness. 0.75 μm) were obtained by capturing serial images of the xy planes by varying the focal length of the same to image consecutive z-axis. The LSM picture files were analyzed using Image *J* software.

2.8. Mitochondrial localization

Localization in mitochondria was visualized by confocal laser scanning microscopy. HeLa cells were grown on cover slips placed in 6-well tissue culture plates until they reached 60–70% confluency. The cells were then incubated with FITC-labeled dendrimers (1 μM) for 4 h in the serum-free media. Mitotracker deep red (100 nM) for 30 min and Hoechst 33342 (5 μg/mL) for 5 min were added prior to washing the cells thoroughly to remove dendrimer, Mitotracker and DNA stain all together. The cells were fixed with 4% p-formaldehyde for 15 min. The cover slips were mounted cell-side-down on glass slides with fluoromount G media and visualized with a confocal laser scanning microscopy with DAPI (ex. 385 nm, em. 470 nm), FITC (ex. 505 nm, em. 530 nm) and Mitotracker deep red (ex. 644 nm, em. 665 nm) filter sets. Fluorescent micrographs of red, green and blue channels were overlaid so that the co-localization of the green fluorescence of dendrimers with the deep red fluorescence of stained mitochondria was rendered as yellow.

2.9. Cytotoxicity

Cytotoxicity of the dendrimers and modified dendrimers were determined with a CellTiter 96® AQueous One Solution Cell Proliferation Assay kit following the manufacturer's protocol. Briefly, all the cells for cytotoxicity experiment were seeded in 96-well tissue culture plates at 5×10^3/well. The next day, the cells were incubated with G(5)-D, G(5)-D-Ac and G(5)-D-Ac-TPP at varying concentrations for 24 and 48 h. At the end of the incubation period, the cells were washed with PBS and supplemented with 100 μL of the serum-free DMEM followed by the addition of 20 μL of Cell Titer Blue Assay Reagent. The cells were incubated with the reagent for 2 h. The fluorescence intensitywas measured by a multi-detection microplate reader (Biotek, Winooski, VT) using 530/590 ex/em wavelengths. Cells treated with only medium were considered 100% viable.

2.10. Statistical analysis

All numerical *in vitro* data are expressed as mean ± SD, $n = 3$. The data were analyzed for statistical significance using the paired Student's T-test using GraphPad prism 5 (GraphPad Software, Inc.; San Diego, CA). Any p value less than 0.05 was considered statistically significant.

3. Results

3.1. Synthesis, purification and characterization of modified dendrimers

The TPP groups were successfully introduced on the dendrimer surface by activated acid-amine coupling reaction following Scheme 1. Reaction of FITC-NHS with G(5)-D at 1:1 M ratio yielded FITC-G(5)-D as orange-yellow solid. The reaction was rapid, spontaneous and high yielding where the NHS-activated acid group of FITC-NHS reacted readily with the primary amine group of the G(5)-D. The dialysis of the reaction mixture using a cellulose ester membrane MWCO 10 kDa removed small molecule impurities. Reaction of FITC-G(5)-D with 90 M excess of acetic anhydride in presence of base TEA yielded partially acetylated FITC-G(5)-D-Ac. This reaction was spontaneous, therefore maintaining stoichiometry was important for avoiding over-acetylation. The reaction of TPP-conjugation on FITC-G(5)-D-Ac using 5 M excess of NHS-activated CTPB resulted attachment of two TPP groups on the surface. The synthesized molecules were characterized by NMR spectroscopy and MALDI–TOF mass spectrometry. The characteristic peaks noted at different PPM values are as follows (where singlet, multiplate, broad and sharp singlets are noted as s, m, b and ss, respectively): For G(5)-D, ^{1}H-NMR in DMSO. δ 5 2.2 (s), 2.43 (s), 2.50 (ss), 2.64 (s), 3.1 (bs), 3.48 (ss), 7.94–8.6 (bm, from $-NH_2$ and −NH groups). Addition of FITC was confirmed by MALDI–TOF spectroscopy. For FITC-G(5)-D-Ac, ^{1}H-NMR in

DMSO was as follows: δ 1.79 (ss), 1.90 (ss), 2.18 (s), 2.42 (s), 2.50 (ss), 2.64 (s), 3.10 (s), 3.36 (bs), 7.83–8.00 (m). The conjugation of the acetyl group on the surface resulted in the appearance of a sharp peak in δ 1.79 and δ 1.86 from −COCH_3 groups. For FITC-G(5)-D-Ac-TPP, ^{1}H-NMR in DMSO: δ1.79 (ss), 2.19 (s), 2.42 (s), 2.50 (ss), 2.64 (s), 3.10 (s), 3.39 (bs), 7.85–7.97 (m). The change in the multiplate peaks in the deshielded aromatic peaks at δ 7.85–7.97 indicated the conjugation of the phenyl groups.

From the MS spectra (Fig. 1), the average molecular weight of G(5)-D was 26425, which was lower than the reported molecular weight of 28826 Da. MALDI-TOF spectra of FITC-G(5)-D demonstrated an average molecular weight of 26780 Da, which confirms the attachment of one FITC molecule per dendrimer. Average molecular mass of FITC-G(5)-D-Ac from MALDI–TOF analysis was 30643 Da which indicated that approximately 92 acetyl groups were attached on the surface of the dendrimer. The mass spectra of FITC-G(5)-D-Ac-TPP with an average molecular mass of 31337 Da indicated the functionalization of the dendrimer surface with two TPP groups.

3.2. Dendrimer association with cells by FACS analysis

Flow cytometry analysis was performed to quantify the association of FITC-labeled dendrimers with cells at 1 h and 4 h time points (Fig. 2). The FITC-G(5)-D had the highest cellular association compared to the other functionalized dendrimers, FITC-G(5)-D-Ac and FITC-G(5)-D-Ac-TPP. The representative histogram (Fig. 2A) demonstrated the increase in green fluorescence intensity of HeLa cells treated with dendrimers for 1 h compared to control cells. Cells without treatment were used as a negative control which indicated the auto-fluorescence of the cells. At 1 h, the fluorescence intensity of FITC-G(5)-treated cells was 2.3 and 2.1 times higher than that of the cells treated with the FITC-G(5)-D-Ac and FITC-G(5)-D-Ac-TPP respectively (geometric means of fluorescence for parent, acetylated, and TPP-modified dendrimers were 35.7 ± 1.1, 15.4 ± 0.6 and 16.8 ± 0.5, respectively). The fluorescence of cells treated with FITC-G(5)-D was 18 times higher than the autofluorescence of the cells after 1 h incubation. There was no significant difference between the cell association of FITC-G(5)-D-Ac and FITC-G(5)-D-Ac-TPP at both time points. An increase in fluorescence intensity of cells treated with G(5)-D at 4 h was 1.2 times higher than the fluorescence intensity at 1 h. For cells treated with G(5)-D-Ac and G(5)-D-Ac-TPP the fluorescence was 1.5 and 1.4 times higher, respectively, at 4 h compared to 1 h of treatment.

3.3. Cellular uptake

Cellular internalization of dendrimers was confirmed and registered by visualization of treated cells as z-stacks of images (images of planes at various focal lengths within the same sample) under confocal laser scanning microscopy (Fig. 3). The z-2–4 and z-10–12 image planes indicated the exterior of the cells. The strong green signal of FITC-G(5)-D-Ac-TPP in the middle slices (z-6 and z-8) indicated the successful internalization, whereas the acetylated precursor dendrimer was moderately internalized and the FITC-G(5)-D was poorly internalized after the 4 h incubation. The cell membrane association of the FITC-G(5)-D and FITC-G(5)-D-Ac was much higher than that for FITC-G(5)-D-Ac-TPP, which gave rise to a strong green background signal in exterior z-slices.

3.4. Mitochondrial localization

To investigate whether FITC-G(5)-D-Ac-TPP was targeting mitochondria, a co-incubation experiment was performed where HeLa cells were treated with FITC-labeled dendrimers, followed by treatment of the cells with Mitotracker deep red and DNA stain Hoechst 33342. Fig. 4 shows the results after HeLa cells were incubated with FITC-labeled G(5)-D, G(5)-D-Ac and G(5)-D-Ac-TPP. The bright field image [Differential Interference Contrast (DIC)] of

the cells is shown to indicate the location of the cells relative to fluorescent signals. Mitochondria were stained with Mitotracker deep red FM, which stains mitochondria in live cells, has a narrow ex/em range (640/662 nm) and its localization in mitochondria depends on the mitochondrial membrane potential. The last panel in the Fig. 4 shows the merged picture, where the co-localization of red signal from Mitotracker and green signal from FITC-labeled dendrimers are rendered yellow to indicate the areas of overlap. Only red and only green signals in the merged picture indicated non-overlapping regions. The assay showed a high degree of co-localization of FITC-G(5)-D-Ac-TPP in mitochondrial compartment (as yellow signal) compared to FITC-G(5)-D and FITC-G(5)-D-Ac. Further evidence of supporting the mitochondrial localization is presented in Fig. 5 where z-stacks of images from red and green fluorescent channels were taken and merged to visualize the colocalization indicated by yellow signal. Higher association between red and green signal (yellow) was evident in the middle slices compared to the exterior slices indicating a true localization of FITC-G(5)-D-Ac-TPP in the mitochondria.

3.5. Cytotoxicity

To explore whether the surface modification imparted for mitochondrial targeting has any effect on the cytotoxicity, a dosedependent cell viability experiment with all three dendrimers was performed in normal mouse fibroblast cell line (NIH-3T3) at 24 and 48 h incubation periods (Fig. 6). Cytotoxicity of the dendrimers was also determined in other cancer cells including HeLa, MCF-7 and 4T1 (Figure S.1). The results demonstrated that the modified dendrimers were significantly less toxic than the starting material G(5)-D. Upon incubation of normal fibroblast cells for 24 h, G(5)-D showed decreased cell viability at ≥ 10 μM. However, no significant cytotoxicity was detected at concentrations tested for G(5)-D-Ac and G(5)-D-Ac-TPP after 24 h incubation. For G(5)-D, all tested doses were cytotoxic after 48 h of incubation whereas G(5)-D-Ac-TPP showed toxicity only at the highest tested concentration (20 μM). G(5)-D-Ac proved to be non-toxic after 24 and 48 h of incubation in tested dose range. The synthesized dendrimers were relatively non-toxic compared to the parent dendrimers towards all the tested cancer cells (Figure S.1). Thus, the modifications of G(5)-D to engineer the mitochondria-targeted G(5)-D-Ac-TPP decreased G(5)-D-associated cytotoxicity.

4. Discussion

Organelle-specific targeting of bio-active molecules is a promising concept to achieve a maximum therapeutic effect and minimum side-effects [18]. Bioactive molecules, if directed specifically towards organelles of interest, such as nucleic acids to the nucleus, pro-apoptotic compounds to the mitochondria or lysosomal drugs or enzymes to the lysosomes, could enhance their therapeutic effect many-fold compared to the random interactions with the desired site of action [25,41–44]. However, directing intracellular trafficking of bio-actives to organelles of interest represents a major challenge for drug delivery. To achieve intracellular targeting, one option has been to modify the drug molecule with organelle-specific ligands. However, this can result in a compromised drug effect. Another option is to modify a nanocarrier to target it to a specific organelle of interest. Mitochondria-targeted DDS have received much attention recently [25,31,35,37,45]. This effort, with emphasis on mitochondrial research, has enabled investigators to identify various small molecules, such as lipophilic cations that target mitochondria [29]. In this regard, the triphenylphosphonium (TPP) cation has been shown to be a potent mitochondriotropic due to its high lipophilicity and stable cationic charge [45]. In another attempt at mitochondrial targeting, peripheral benzodiazepine receptors located in the outer mitochondrial membrane are being explored as a promising mitochondrial drug target for the delivery of anticancer drugs and diagnostic imaging agents to the mitochondria [40,46].

In our attempt to develop a dendrimers as mitochondrial targeted nanocarriers, we conjugated TPP group on their surface. Partial acetylation of the G(5)-D neutralized a fraction of the positive charge on the surface of imparted lipophilicity to the dendrimer. Neutralization of the surface charge of the dendrimer prevented the non-specific interaction and binding of the molecule with cell organelles. Partial acetylation resulted in improved solubility of the acetylated molecules in organic solvents. The solubility is a concern for the conjugation reactions since dendrimers such as G(5)-PAMAM are sparingly soluble in DMF, DMSO and completely insoluble in other organic solvents such as $CHCI_3$. A fraction of the surface amino groups were left un-acetylated for the conjugation of the mitochondria-targeted function TPP. The chemistry following the Scheme 1 allowed the association of two TPP groups on the surface of a single dendrimer using a 5-fold molar excess of CTPB-NHS. MALDI–TOF spectral analysis was confirmatory for the structure of the parent dendrimer and conjugation of small molecules on the surface. A lower than reported molecular weight of the commercially available dendrimer was obtained from the MALDI–TOF spectral analysis. This probably was due to the incomplete reaction in one arm of the dendrimer. Missing a few arms is common in higher generations of dendrimers (G-3, G-4, G-5) and leads to lower molecular weights. Therefore, precise characterization of dendrimers is important for design of the reaction sequence and determining the stoichiometry of other chemicals to be used for the reactions in engineering an efficient nano-device. In this study, we attached functional groups to utilize the reaction capabilities of primary terminal amino groups.

After surface modification of dendrimers, the conjugates were tested in cellular internalization and intracellular trafficking experiments. The flow cytometry data suggest that the surface functionalization has an effect on cell association of dendrimers. The parent dendrimer was highly cationic, resulting in higher association with the anionic cell membrane and its surface proteins. However, the partial surface-charge-neutralization decreased the non-specific interaction with the cell surface and resulted in less association with the cells. Higher uptake of FITC-labeled G(5)-D-Ac-TPP than G(5)-D-Ac was likely to be due to properties imparted by the attachment of the positively charged lipophilic cation, TPP.

Fluorescently labeled dendrimer-dosed cells were visualized with confocal microscopy for assessment of the internalization and mitochondrial localization of the dendrimers. G(5)-D-Ac-TPP demonstrated efficient internalization and a mitochondrial targeting ability. Z-stacked images (pseudoconfocal) allowed regions of the cells to be viewed along the z-axis and confirmed the mitochondrial localization of dendrimers. This technique provided a clear picture of the intracellular environment as the stack of images was acquired since the imaging software controls the precise movement of the motorized focus drive during image acquisition. These results also indicate that the modification of the dendrimer surface with the lipophilic cation TPP significantly enhances intracellular uptake.

Mitochondrial research has established that a compound with sufficient lipophilicity combined with delocalized positive charge will accumulate in the mitochondria [29,47]. The common physicochemical factors underlying selective accumulation of ligands to mitochondria are electric potential, ion trapping, complex formation with cardiolipin, non-specific membrane partitioning and targeting of receptors uniquely that are either expressed or over-expressed in mitochondrial membranes in normal or diseased conditions. The cation TPP has lipophilicity due to the presence of three phenyl groups and a stable delocalized positive charge on the phosphorous that provides many resonance structures due to the movement of electrons in the aromatic region. The TPP has a strong mitochondria-targeting ability, which relies on the mitochondrial membrane potential, and a lipophilic nature suitable for membrane partitioning [29]. The confocal microscopy results provided strong

evidence that TPP-modified dendrimers reach mitochondria. This set of experiments was performed with special attention given to cancer cells since they are likely to be the therapeutic target.

Ideally, any delivery system for biomedical application should be non-toxic for non-target cells. The newly developed dendrimer, G(5)-D-Ac-TPP, were relatively non-toxic to the non-target fibroblast cells, when compared with the parent unmodified dendrimer. Neutralization of surface charge in dendrimer is necessary to reduce non-specific interactions which leads to cytotoxicity [48–51]. However, a balance between tertiary amines formed after ligand-conjugation and unconjugated primary amines in dendrimer is necessary for efficient cellular internalization and endosomal escape. Many possibilities using conjugation chemistry should allow modified dendrimers to be designed for therapeutic needs.

5. Conclusions

A mitochondria-targeted, relatively non-toxic pharmaceutical nanocarrier, G(5)-D-Ac-TPP, was developed. Conjugation of a mitochondriotropic TPP group with the surface of this dendrimer imparted a mitochondria-targeting property, whereas the acetylation partially neutralizes the positive charge on the surface of the dendrimer. Mitochondria are emerging as a promising pharmacological target for anticancer, anti-obesity, anti-oxidant and gene therapy, since numerous metabolic pathways are directly or indirectly associated with mitochondrial function. This non-toxic mitochondria-targeted nanocarrier represents an effective vehicle for efficient delivery of a therapeutic cargo with loading of bioactive agents in the dendrimer core by an electrostatic interaction or by surface conjugation. This dendrimer-based carrier, G(5)-D-Ac-TPP, efficiently targets mitochondria and decreases the non-target toxicity typically associated with dendrimers. Further investigations are in progress to demonstrate that mitochondria-targeted dendrimers can carry and successfully deliver a therapeutic payload to the mitochondria.

Supplementary Material

Refer to Web version on PubMed Central for supplementary material.

Acknowledgments

The work was supported by the NIH grants R01 CA 121838 and R01 CA 128486 to Vladimir P. Torchilin. We thank Dr. William Hartner for his helpful advice in editing the manuscript.

References

1. Cheng Y, Wang J, Rao T, He X, Xu T. Pharmaceutical applications of dendrimers: promising nanocarriers for drug delivery. Front Biosci. 2008; 13:1447–1471. [PubMed: 17981642]
2. Caminade AM, Laurent R, Majoral JP. Characterization of dendrimers. Adv Drug Deliv Rev. 2005; 57(15):2130–2146. [PubMed: 16289434]
3. Dufes C, Uchegbu IF, Schatzlein AG. Dendrimers in gene delivery. Adv Drug Deliv Rev. 2005; 57(15):2177–2202. [PubMed: 16310284]
4. Tomalia DA, Reyna LA, Svenson S. Dendrimers as multi-purpose nanodevices for oncology drug delivery and diagnostic imaging. Biochem Soc Trans. 2007; 35(Pt 1):61–67. [PubMed: 17233602]
5. Portney NG, Ozkan M. Nano-oncology: drug delivery, imaging, and sensing. Anal Bioanal Chem. 2006; 384(3):620–630. [PubMed: 16440195]
6. Bremer C, Ntziachristos V, Weissleder R. Optical-based molecular imaging: contrast agents and potential medical applications. Eur Radiol. 2003; 13(2):231–243. [PubMed: 12598985]

7. Gillies ER, Frechet JM. Dendrimers and dendritic polymers in drug delivery. Drug Discov Today. 2005; 10(1):35–43. [PubMed: 15676297]
8. Svenson S, Tomalia DA. Dendrimers in biomedical applications-reflections on the field. Adv Drug Deliv Rev. 2005; 57(15):2106–2129. [PubMed: 16305813]
9. Gao Y, Gao G, He Y, Liu T, Qj R. Recent advances of dendrimers in delivery of genes and drugs. Mini Rev Med Chem. 2008; 8(9):889–900. [PubMed: 18691146]
10. Tang MX, Redemann CT, Szoka FC Jr. In vitro gene delivery by degraded polyamidoamine dendrimers. Bioconjug Chem. 1996; 7(6):703–714. [PubMed: 8950489]
11. Haensler J, Szoka FC Jr. Polyamidoamine cascade polymers mediate efficient transfection of cells in culture. Bioconjug Chem. 1993; 4(5):372–379. [PubMed: 8274523]
12. Singha K, Namgung R, Kim WJ. Polymers in small-interfering RNA delivery. Nucleic Acid Ther. 2011; 21(3):133–147. [PubMed: 21749290]
13. Yuan X, Naguib S, Wu Z. Recent advances of siRNA delivery by nanoparticles. Expert Opin Drug Deliv. 2011; 8(4):521–536. [PubMed: 21413903]
14. Bielinska AU, Kukowska-Latallo JF, Baker JR Jr. The interaction of plasmid DNA with polyamidoamine dendrimers: mechanism of complex formation and analysis of alterations induced in nuclease sensitivity and transcriptional activity of the complexed DNA. Biochim Biophys Acta. 1997 Aug 7; 1353(2):180–190. [PubMed: 9294012]
15. Choi YS, Cho TS, Kim JM, Han SW, Kim SK. Amine terminated G-6 PAMAM dendrimer and its interaction with DNA probed by Hoechst 33258. Biophys Chem. 2006; 121(2):142–149. [PubMed: 16458415]
16. Bielinska AU, Chen C, Johnson J, Baker JR Jr. DNA complexing with polyamidoamine dendrimers: implications for transfection. Bioconjug Chem. 1999; 10(5):843–850. [PubMed: 10502352]
17. Richardson SC, Pattrick NG, Man YK, Ferruti P, Duncan R. Poly(amidoamine)s as potential nonviral vectors: ability to form interpolyelectrolyte complexes and to mediate transfection in vitro. Biomacromolecules. 2001; 2(3):1023–1028. [PubMed: 11710005]
18. Torchilin VP. Recent approaches to intracellular delivery of drugs and DNA and organelle targeting. Annu Rev Biomed Eng. 2006; 8:343–375. [PubMed: 16834560]
19. Patil ML, Zhang M, Minko T. Multifunctional triblock nanocarrier (PAMAM-PEG-PLL) for the efficient intracellular siRNA delivery and gene silencing. ACS Nano. 2011; 5(3):1877–1887. [PubMed: 21322531]
20. Yamada Y, Akita H, Kogure K, Kamiya H, Harashima H. Mitochondrial drug delivery and mitochondrial disease therapyan approach to liposome-based delivery targeted to mitochondria. Mitochondrion. 2007; 7(1–2):63–71. [PubMed: 17296332]
21. Schon EA, DiMauro S. Medicinal and genetic approaches to the treatment of mitochondrial disease. Curr Med Chem. 2003; 10(23):2523–2533. [PubMed: 14529468]
22. Holt IJ, Harding AE, Morgan-Hughes JA. Deletions of muscle mitochondrial DNA in patients with mitochondrial myopathies. Nature. 1988; 331(6158):717–719. [PubMed: 2830540]
23. Wallace DC. Mitochondrial diseases in man and mouse. Science. 1999 Mar 5; 283(5407):1482–1488. [PubMed: 10066162]
24. Liu X, Kim CN, Yang J, Jemmerson R, Wang X. Induction of apoptotic program in cell-free extracts: requirement for dATP and cytochrome c. Cell. 1996; 86(1):147–157. [PubMed: 8689682]
25. Fulda S, Galluzzi L, Kroemer G. Targeting mitochondria for cancer therapy. Nat Rev Drug Discov. 2010; 9(6):447–464. [PubMed: 20467424]
26. Wallace DC, Singh G, Lott MT, Hodge JA, Schurr TG, Lezza AM, et al. Mitochondrial DNA mutation associated with Leber's hereditary optic neuropathy. Science. 1988; 242(4884):1427–1430. [PubMed: 3201231]
27. Adlam VJ, Harrison JC, Porteous CM, James AM, Smith RA, Murphy MP, et al. Targeting an antioxidant to mitochondria decreases cardiac ischemia-reperfusion injury. FASEB J. 2005; 19(9): 1088–1095. [PubMed: 15985532]
28. Jauslin ML, Meier T, Smith RA, Murphy MP. Mitochondria-targeted antioxidants protect Friedreich Ataxia fibroblasts from endogenous oxidative stress more effectively than untargeted antioxidants. FASEB J. 2003; 17(13):1972–1974. [PubMed: 12923074]

29. Horobin RW, Trapp S, Weissig V. Mitochondriotropics: a review of their mode of action, and their applications for drug and DNA delivery to mammalian mitochondria. J Control Release. 2007 Aug 28; 121(3):125–136. [PubMed: 17658192]
30. Pupure J, Isajevs S, Skapare E, Rumaks J, Svirskis S, Svirina D, et al. Neuroprotective properties of mildronate, a mitochondria-targeted small molecule. Neurosci Lett. 2010; 470(2):100–105. [PubMed: 20036318]
31. Boddapati SV, D'Souza GG, Erdogan S, Torchilin VP, Weissig V. Organelle-tar-geted nanocarriers: specific delivery of liposomal ceramide to mitochondria enhances its cytotoxicity in vitro and in vivo. Nano Lett. 2008; 8(8):2559–2563. [PubMed: 18611058]
32. Boddapati SV, Tongcharoensirikul P, Hanson RN, D'Souza GG, Torchilin VP, Weissig V. Mitochondriotropic liposomes. J Liposome Res. 2005; 15(1—2):49–58. [PubMed: 16194927]
33. Biswas S, Dodwadkar NS, Sawant RR, Koshkaryev A, Torchilin VP. Surface modification of liposomes with rhodamine-123-conjugated polymer results in enhanced mitochondrial targeting. J Drug Target. 2011; 19(7):552–561. [PubMed: 21348804]
34. Patel NR, Hatziantoniou S, Georgopoulos A, Demetzos C, Torchilin VP, Weissig V, et al. Mitochondria-targeted liposomes improve the apoptotic and cytotoxic action of sclareol. J Liposome Res. 2010; 20(3):244–249. [PubMed: 19883213]
35. Flierl A, Jackson C, Cottrell B, Murdock D, Seibel P, Wallace DC. Targeted delivery of DNA to the mitochondrial compartment via import sequence-conjugated peptide nucleic acid. Mol Ther. 2003; 7(4):550–557. [PubMed: 12727119]
36. D'Souza GG, Rammohan R, Cheng SM, Torchilin VP, Weissig V. DQAsome-mediated delivery of plasmid DNA toward mitochondria in living cells. J Control Release. 2003; 92(1–2):189–197. [PubMed: 14499196]
37. Cuchelkar V, Kopeckova P, Kopecek J. Novel HPMA copolymer-bound constructs for combined tumor and mitochondrial targeting. Mol Pharm. 2008; 5(5):776–786. [PubMed: 18767867]
38. Diers AR, Higdon AN, Ricart KC, Johnson MS, Agarwal A, Kalyanaraman B, et al. Mitochondrial targeting of the electrophilic lipid 15-deoxy-Deltal2,14-prostaglandin J2 increases apoptotic efficacy via redox cell signalling mechanisms. Biochem J. 2010; 426(1):31–41. [PubMed: 19916962]
39. Kelso GF, Porteous CM, Coulter CV, Hughes G, Porteous WK, Ledgerwood EC, et al. Selective targeting of a redox-active ubiquinone to mitochondria within cells: antioxidant and antiapoptotic properties. J Biol Chem. 2001; 276(7):4588–4596. [PubMed: 11092892]
40. Samuelson LE, Dukes MJ, Hunt CR, Casey JD, Bornhop DJ. TSPO targeted dendrimer imaging agent: synthesis, characterization, and cellular internalization. Bioconjug Chem. 2009; 20(1l): 2082–2089. [PubMed: 19863077]
41. Shi F, Hoekstra D. Effective intracellular delivery of oligonucleotides in order to make sense of antisense. J Control Release. 2004; 97(2):189–209. [PubMed: 15196747]
42. Stefano JE, Hou L, Honey D, Kyazike J, Park A, Zhou Q, et al. In vitro and in vivo evaluation of a non-carbohydrate targeting platform for lysosomal proteins. J Control Release. 2009; 135(2):113–118. [PubMed: 19146893]
43. Won YW, Lim KS, Kim YH. Intracellular organelle-targeted non-viral gene delivery systems. J Control Release. 2011; 152(1):99–109. [PubMed: 21255626]
44. Jensen KD, Nori A, Tijerina M, Kopeckova P, Kopecek J. Cytoplasmic delivery and nuclear targeting of synthetic macromolecules. J Control Release. 2003; 87(1–3):89–105. [PubMed: 12618026]
45. Hoye AT, Davoren JE, Wipf P, Fink MP, Kagan VE. Targeting mitochondria. Ace Chem Res. 2008; 41(1):87–97.
46. Laquintana V, Denora N, Musacchio T, Lasorsa M, Latrofa A, Trapani G. Peripheral benzodiazepine receptor ligand-PLGA polymer conjugates potentially useful as delivery systems of apoptotic agents. J Control Release. 2009; 137(3):185–195. [PubMed: 19374931]
47. Smith RA, Porteous CM, Gane AM, Murphy MP. Delivery of bioactive molecules to mitochondria in vivo. Proc Natl Acad Sci U S A. 2003; 100(9):5407–5412. [PubMed: 12697897]

48. Wang Y, Guo R, Cao X, Shen M, Shi X. Encapsulation of 2-methoxyestradiol within multifunctional poly(amidoamine) dendrimers for targeted cancer therapy. Biomaterials. 2011; 32(12):3322–3329. [PubMed: 21315444]

49. Shan Y, Luo T, Peng C, Sheng R, Cao A, Cao X, et al. Gene delivery using dendrimer-entrapped gold nanoparticles as nonviral vectors. Biomaterials. 2012; 33(10):3025–3035. [PubMed: 22248990]

50. Shi X, Lee I, Chen X, Shen M, Xiao S, Zhu M, et al. Influence of dendrimer surface charge on the bioactivity of 2-methoxyestradiol complexed with dendrimers. Soft Matter. 2010; 6(11):2539–2545. [PubMed: 20852741]

51. Peng C, Zheng L, Chen Q, Shen M, Guo R, Wang H, et al. PEGylated dendrimer-entrapped gold nanoparticles for in vivo blood pool and tumor imaging by computed tomography. Biomaterials. 2012; 33(4):1107–1119. [PubMed: 22061490]

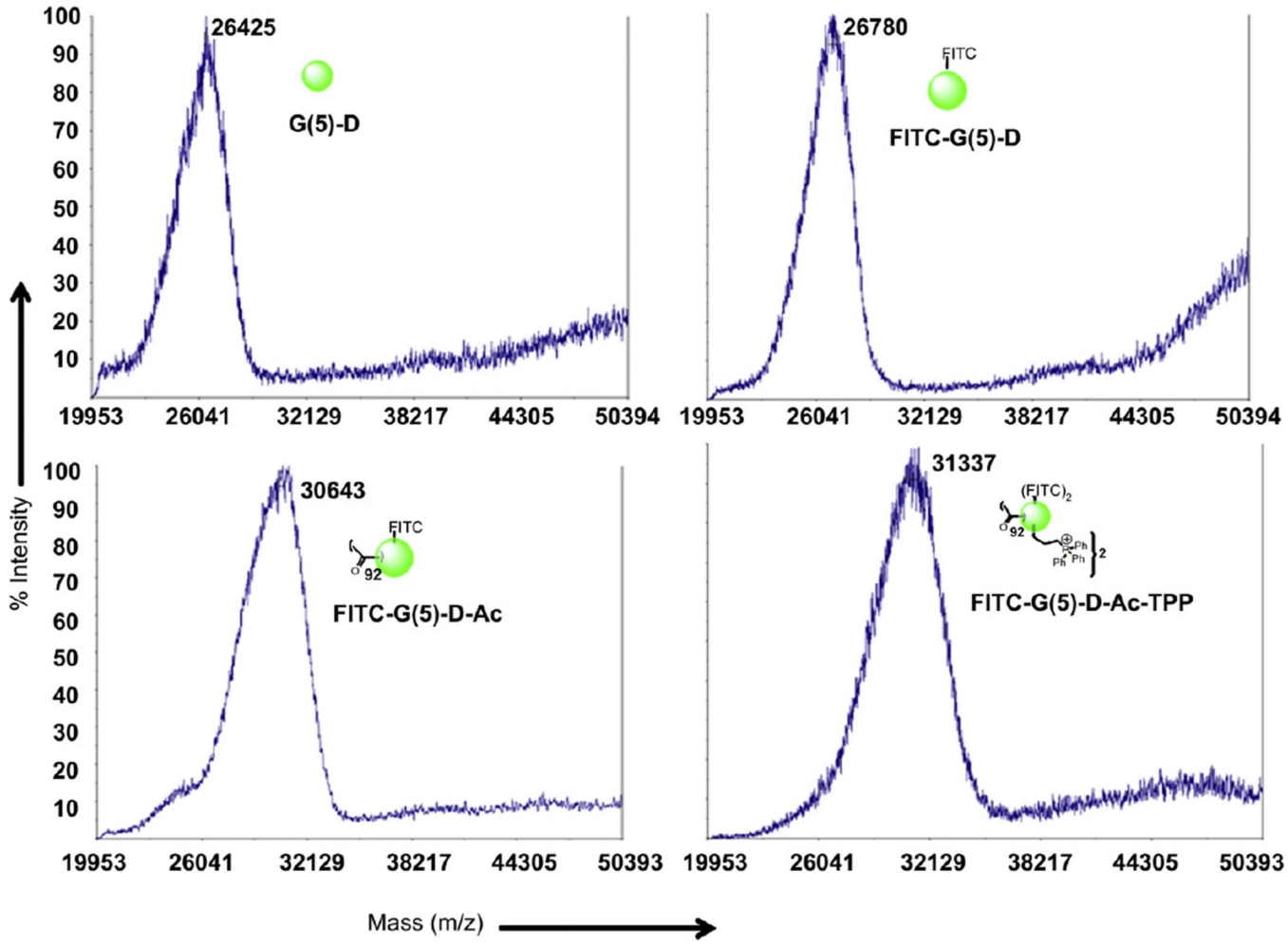

Fig. 1.

Characterization of dendrimers by MALDI–TOF mass spectroscopy. A. MALDI–TOF spectrum of the starting material G(5)-PAMAM dendrimer; B. MALDI–TOF spectra of FITC-labeled G(5)-PAMAM dendrimer; C. MALDI–TOF spectra of acetylated FITC-labeled PAMAM dendrimer. D. MALDI-TOF spectra of TPP-conjugated FITC-labeled acetylated G(5)-PAMAM dendrimer.

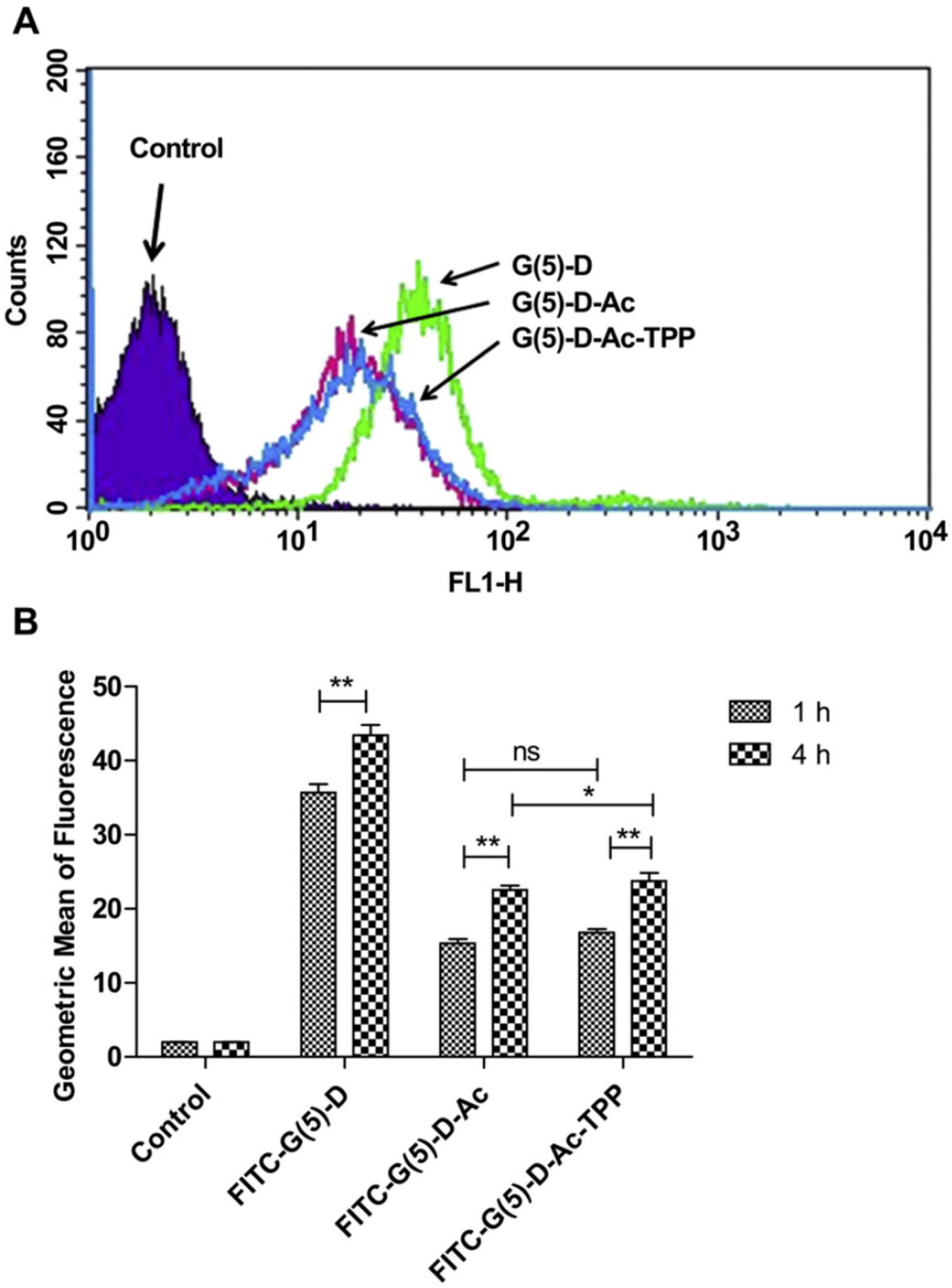

Fig. 2.

Cell-association of dendrimers by flow cytometric analysis. A. A representative histogram showing the change in FITC-fluorescence intensity of HeLa cells treated with FITC-labeled FITC-G(5)-D, FITC-G(5)-D-Ac and FITC-G(5)-D-Ac-TPP (0.5 μM) for 1 h compared to untreated cells (control). B. FITC-fluorescence intensities of cells treated with specified dendrimers at different incubation time (1 h and 4 h). Untreated cells were used as control for each corresponding incubation time. Data expressed as mean ± SD of three experiments carried out in triplicates (*$p < 0.05$ and **$p < 0.001$).

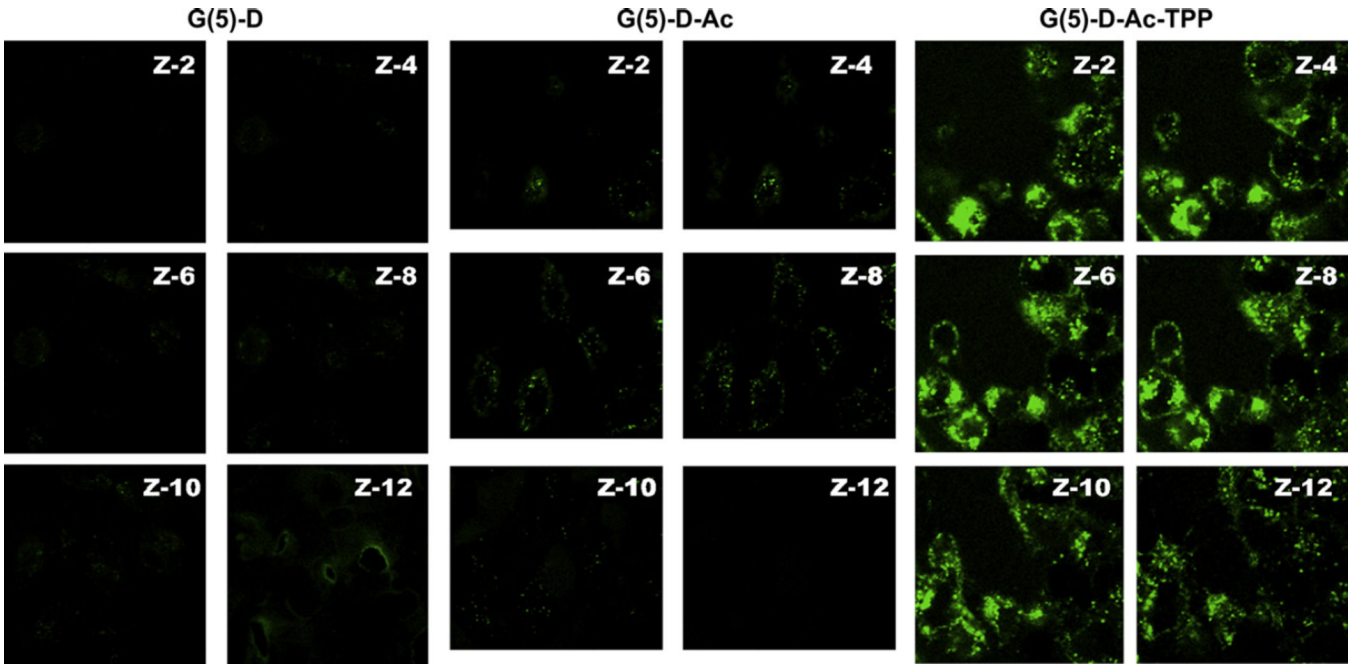

Fig. 3.

Intracellular uptake of dendrimers in HeLa cells visualized by confocal microscopy. Green fluorescence images of cells were taken after the incubation with FITC-labeled dendrimers (1.0 μM) for 4 h using laser 490 nm (Left panel. G(5)-D, middle panel. G(5)-D-Ac and right panel. G(5)-D-Ac-TPP). Serial images of the xy planes (z-slice) (z-2 to z-12) of the same cells were taken at consecutive z-axis slices of 0.75 μm.

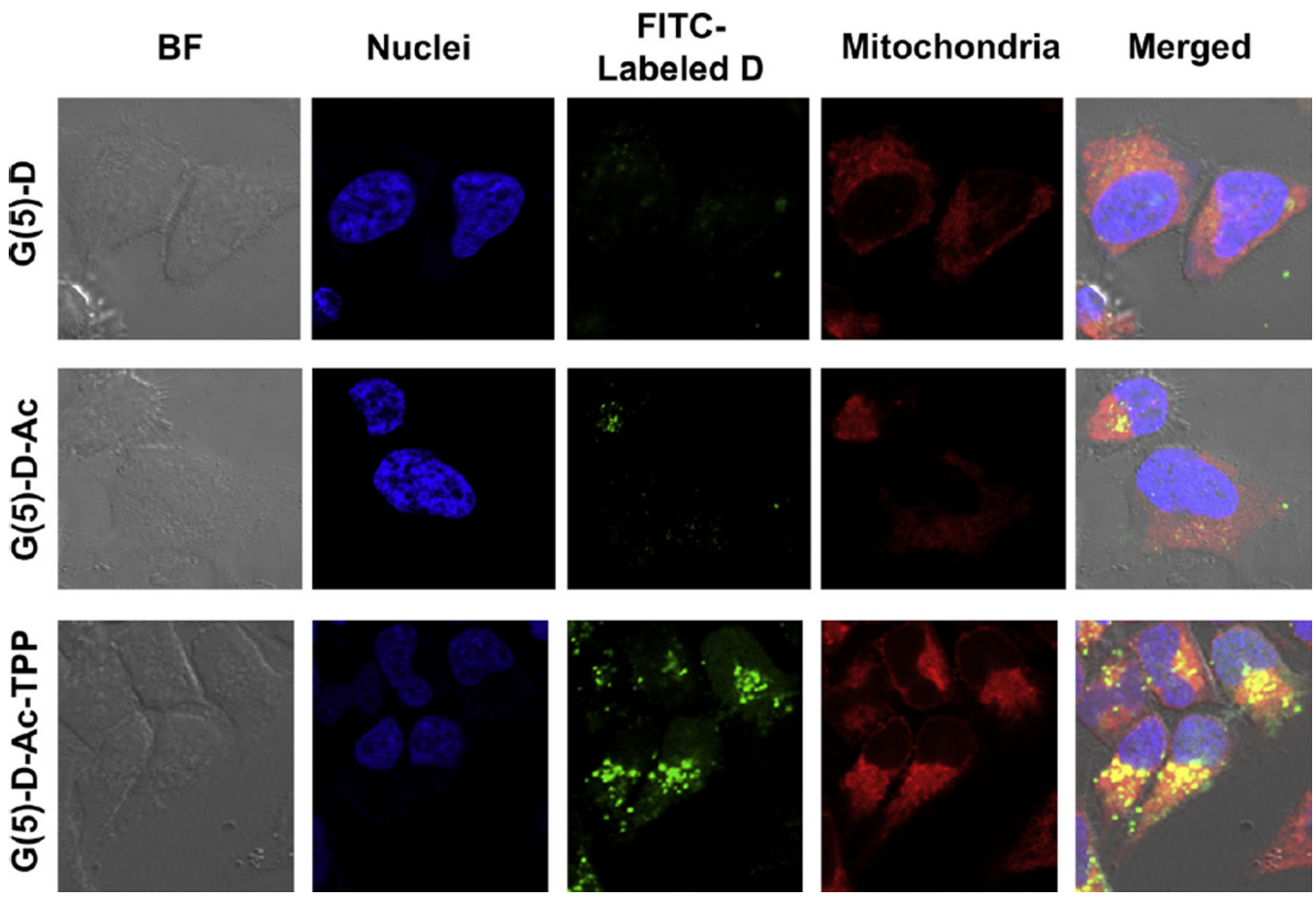

Fig. 4.

Mitochondrial localization of FITC-Labeled dendrimers in HeLa cells by confocal laser scanning microscopy. Cells were treated with Hoechst 33342 for nuclei and Mitotracker deep red for mitochondrial staining and viewed in the blue channel for Hoechst (ex. 385 nm, em. 470 nm), the green channel for FITC (ex. 505 nm, em. 530 nm) and the red channel for Mitotracker deep red (ex. 640 nm, em. 662 nm). Yellow spots in the merged images arising from the co-localization of deep red and green signal indicate mitochondrial localization of dendrimers.

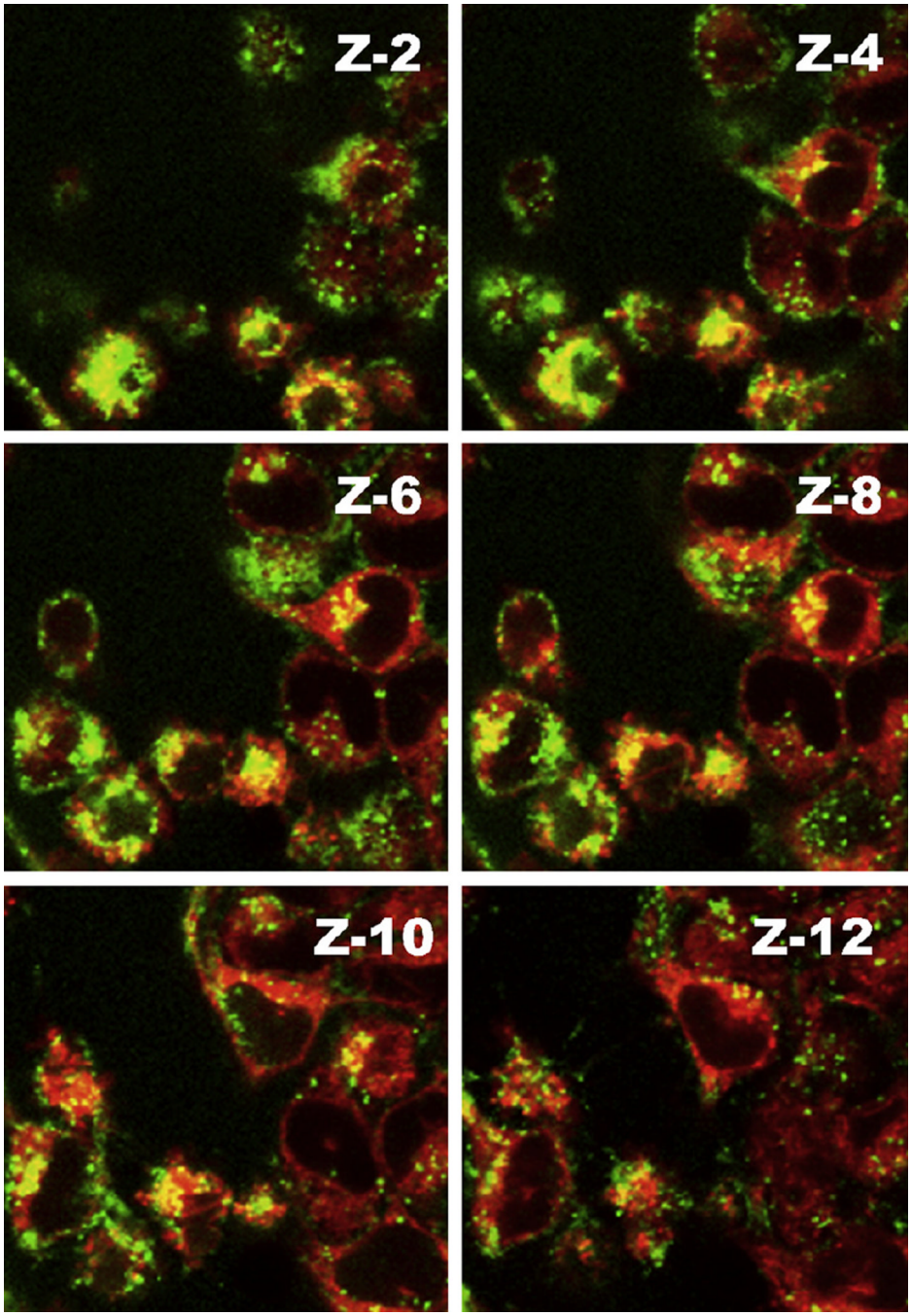

Fig. 5.

The mitochondrial localization of FITC-G(5)-D-Ac-TPP assessed by co-localized fluorescence signal from stained mitochondria and dendrimer visualized with confocal laser scanning microscope of z-stacked images. Mitochondria were stained with Mitotracker deep red and dendrimers were labeled with FITC. The yellow spots indicate co-localization of green and red signals. Serial images of the xy planes (z-slice) (z-2 to z-12 out of 15 slices) of the same cells were taken along the z-axis at slice thicknesses of 0.75 μm to assess the intracellular trafficking of dendrimers to mitochondria.

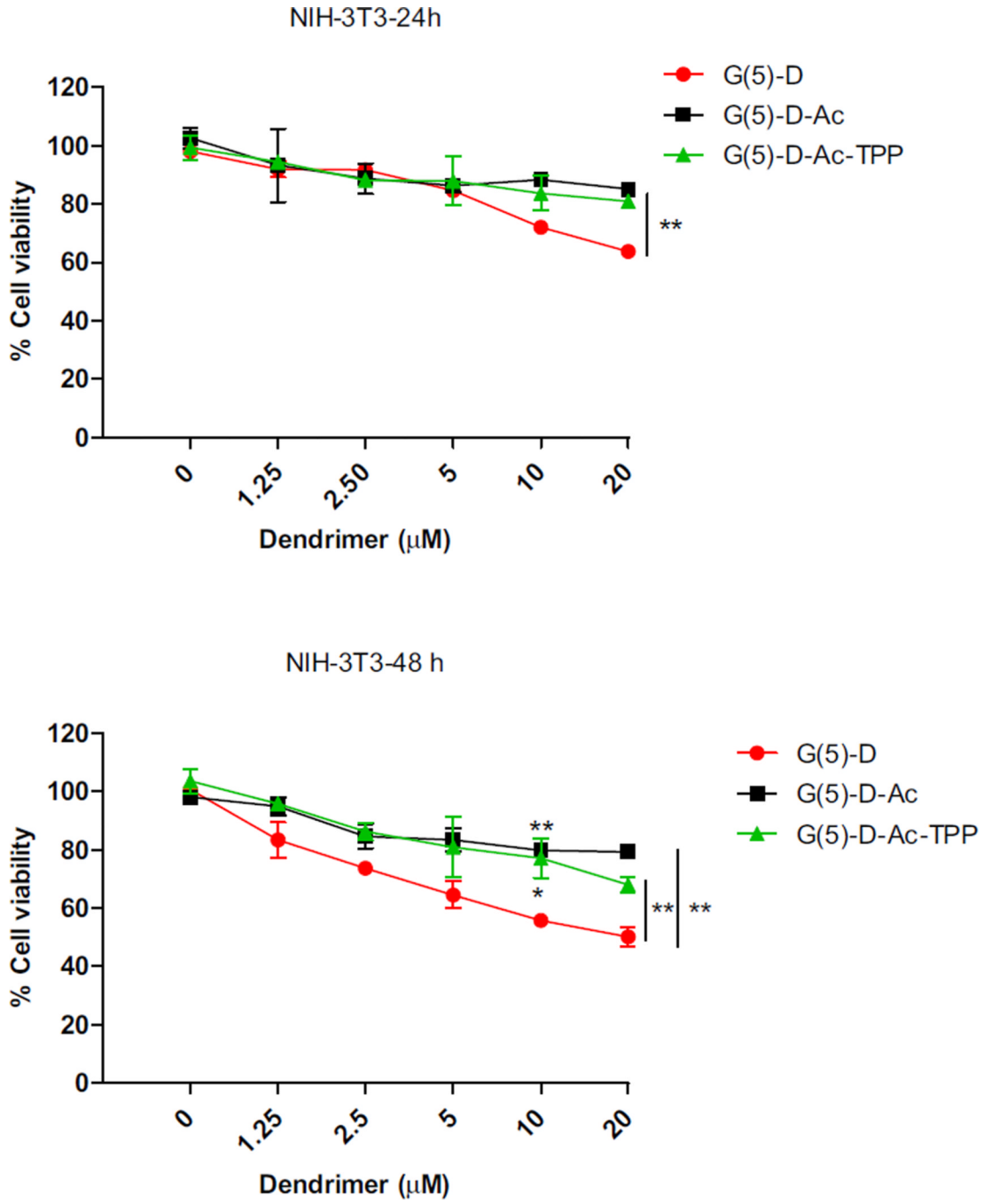

Fig. 6.

Dose-dependent cytotoxicity of dendrimers against NIH-3T3 cells at 24 and 48 h. Data are expressed as mean ± SD of three experiments carried out in triplicate. Difference between G(5)-D and G(5)-D-Ac/G(5)-D-Ac-TPP were analyzed by Student's T-test. (*$p < 0.05$ and **$p < 0.01$).

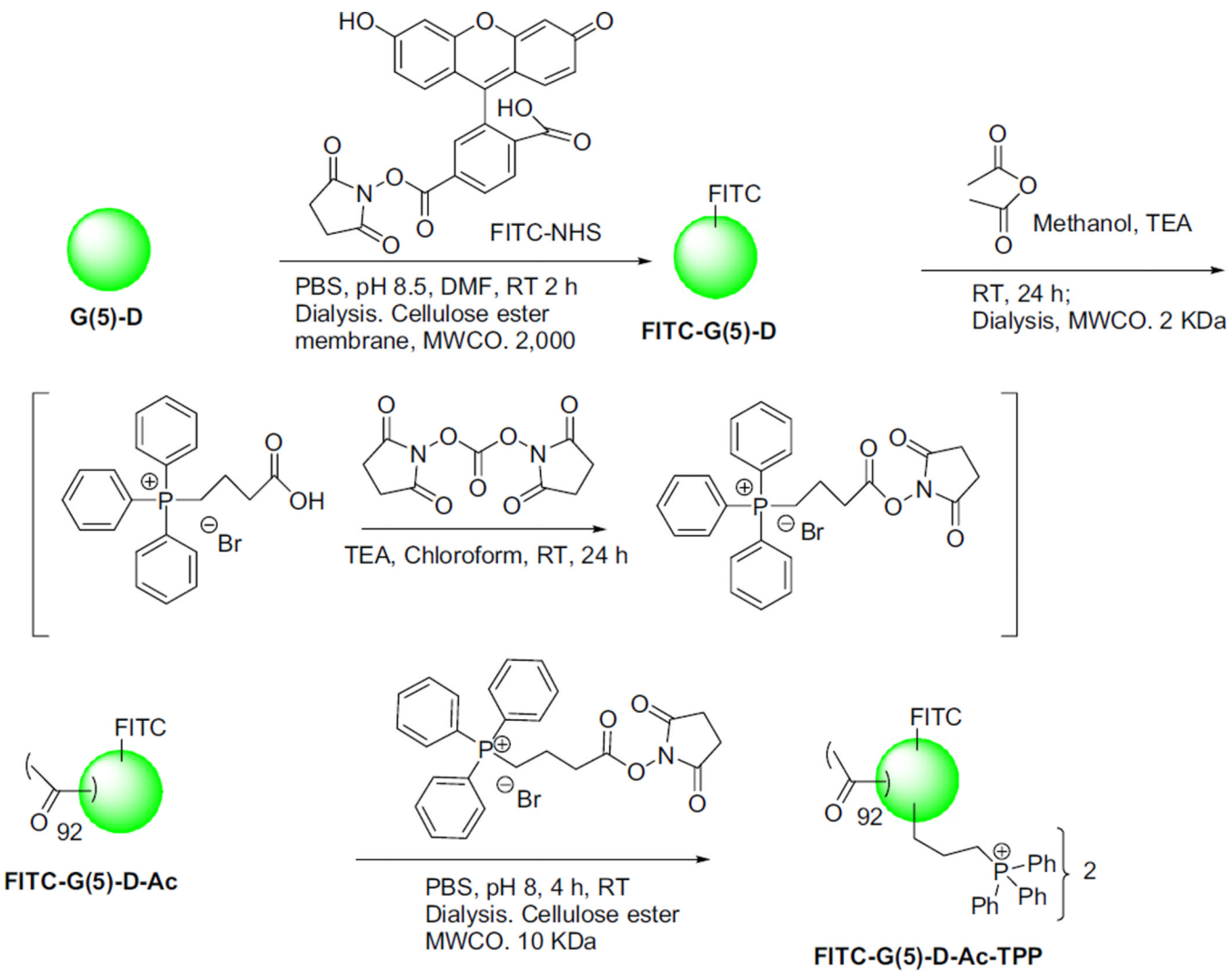

Scheme 1.
Synthesis of TPP-conjugated, fluorescently-labeled, acetylated G(5)-PAMAM dendrimer.